# IMPROVEMENT IN ORIENTATION MEASUREMENT FOR SHORT AND LONG FIBER INJECTION MODLED COMPOSITES

*G. M. Vélez-Garcia[1], S. Mazahir[1], J. Hofmann[1], P., Wapperom[1], D. Baird[1], A. Zink-Sharp[1], V. Kunc[2]*

*[1]Virginia Tech, Blacksbrug, VA, 24061*
*[2]Oak Ridge National Laboratory, Oak Ridge, TN, 37831*

## Abstract

Short and long fiber reinforced thermoplastics are a feasible alternative to develop lightweight materials for semi-structural and structural applications, respectively. These composites present a layered structure showing a complex tridimensional structure along the molding, created during the forming stage. The details of short fiber orientation in a center-gated disk with diameter of 1.38 mm were obtained in several regions including the gate and advancing front. Several modifications were introduced in the method of ellipses to obtain unambiguous orientation of 30 % short glass-fiber PBT. The unambiguous $A_{r\theta}$ component was successfully obtained with the modified method. The results also showed an asymmetric distribution of fiber orientation that gradually washout as the flow progress. In addition, the initial orientation measured at the gate presented a fiber distribution different from the random orientation that is assumed in literature for a center-gated disk. Additionally, the initial results of this modified method to assess the complex structure of a 30 % long glass-fiber PP end-gated plaque are shown.

## Background

Short and long fiber composites have generated commercial interest in the manufacturing of lightweight parts used in semi-structural and structural applications, respectively. The improved mechanical properties in these materials are defined by the tridimensional structure of the fibers, established mainly during the forming stage of the parts due to the flow-induced orientation. In the case of short fibers (i.e. $l$ < 1 mm, where l denotes the length of the fiber), they are rigid particles and the structure is well characterized by simply the orientation of the fibers. In the case of long fibers i.e. $l$ > 1 mm, their characterization is more complex due to the semi-flexibility of the fibers given by its length. However, a reliable and cost-effective experimental method to quantify the final three-dimensional (3D) orientation state in short fibers and account for the semi-flexibility description of long fibers, is not available.

The evaluation of the internal structure in short fibers is easier and mature when compared with the long fibers. Optical[1] and irradiation[2] methods are the standard methods to evaluate the fiber orientation of short and long fibers, respectively. A complete review of additional methods can be seen elsewhere[3]. The optical methods use two-dimensional (2D) data and stereological principles to obtain an incomplete 3D description of orientation within the part. This incompleteness in orientation can be attributed to the geometrical limitations inherent to the 2D method used to quantify the orientation, known as the method of ellipses[3]. This limitation is commonly referred to as an ambiguity problem because one of the angles used to describe the fiber orientation cannot be determined unambiguously[3]. In spite of this limitation, the simplicity and reduced cost has made the method of ellipses, the preferred method to evaluate fiber orientation.

The irradiation methods used in the characterization of long fibers are non-destructive techniques able to give a complete 3D representation of the orientation. However, these methods require extremely expensive equipment, which has limited their applications in detailed and complete studies[4]. Recently, based on the assumption of rigid long fibers, the method of ellipses have been used to characterize long fibers in several positions of end-gated[5] and center-gated[6] molded parts.

In the last 15 years, several experimental techniques claiming the elimination of the ambiguity have been developed [3,7]. One of these techniques claimed a simple solution of the problem using a method named shadow - scanning electron microscopy (SEM) introduced by Averous [8] and recently used by Reginer et al. [9]. However, use of SEM increases the cost and problems associated with SEM. Therefore, an analogous approach based on the shadow tracking method is proposed here. The advantage of the proposed method is the use of reflection optical microscopy to acquire the micrograph. This has the benefits of cost reduction and greater simplicity of the method. The correct direction of the fiber is determined based on the location of a shadow at an extremity of the ellipse.

The objective of this paper is to develop a simple and unambiguous method to obtain the tridimensional structure of short and long fibers in fiber reinforced composites. Firstly, the elimination of the ambiguity problem is addressed by introducing simple and inexpensive modifications to the method of ellipses. Secondly, the modified method of ellipses is extended to capture the bending of the long fibers. In the new procedure, the semi-flexibility of the fiber is obtained by constructing a tridimensional end-to-end vector based on the elliptical footprints found in multiple planes evaluated through the thickness of the part. The initial results of this approach to determine the structure of long fibers are shown.

## Description of Fiber Orientation in Composites

A short fiber is assumed as a cylindrical, rigid, straight rod. Therefore, its spatial orientation can be described using spherical coordinates with the azimuthal ($\phi$) and zenith ($\theta$) angles as is shown in Fig. 1. These angles are used to construct an orientation unit vector **p** parallel to the backbone of the particle defined as

$$\mathbf{p} = p_1\boldsymbol{\delta}_1 + p_2\boldsymbol{\delta}_2 + p_3\boldsymbol{\delta}_3 \tag{1}$$

where the components are defined as:

$$p_1 = \sin\theta\cos\phi \quad p_2 = \sin\theta\sin\phi \quad p_3 = \cos\theta \tag{2}$$

The orientation of a population of fibers can be described using orientation tensors, as proposed by Advani and Tucker [10]. The second order orientation tensor (**A**) is the most widely used tensor representation of the orientation state in the thermoplastic composite literature.

$$\mathbf{A} = A_{ij} = \left\langle p_i p_j \right\rangle \tag{3}$$

where $\left\langle \_ \right\rangle$ represents the ensemble average of the dyadic product of the unit vector **p** over all possible orientations at a certain position and time. Experimentally, the unbiased weighted-average second-rank orientation tensor is computed by [11]

$$\bar{A}_{ij} = \frac{\sum \left(A_{ij}\right)_n F_n}{\sum F_n} \tag{4}$$

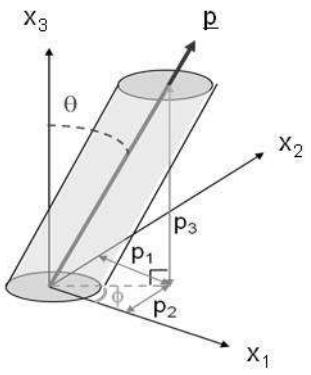


*Figure 1. Orientation components for a single fiber description.*

where $F_n$ is a volumetric weighting function used to transform the orientation measured over the polished plane into the volume of the composite. The simplest and commonly used weighting function is described by Bay and Tucker[11]. In this model the correction is inversely proportional to projected fiber surface [12] and is described by

$$F_n = \begin{cases} \dfrac{1}{L_n \cos\theta_n} & \theta \le \cos^{-1}\left(a_r^{-1}\right) \\ \dfrac{1}{d_n} & \theta > \cos^{-1}\left(a_r^{-1}\right) \end{cases} \tag{5}$$

where $d_n$ is the diameter of the *n-th* fiber $a_r$ is the aspect ratio.

## Method of Ellipses

The method of ellipses[3] is a 2D technique commonly used to characterize orientation in short fiber composites. A specimen taken from a region of interest in a composite is cut, mounted, and polished using common metallographic techniques. The sample is plasma etched for a long time and gold sputtered to increase the contrast between the matrix and fibers. Then a reflective optical microscope is used to acquire the images of the surface of the sample[13]. The resulting image has multiple elliptical footprints representing fibers cut by the surface plane of the polished sample.

Five geometrical parameters are measured from each ellipse and subsequently used to construct the vector of orientation. Fig. 2 can help to visualize the parameters directly measured from each ellipse. The fiber position is determined from the horizontal and vertical center of mass ($h_c$, $v_c$) of the ellipse. The remaining parameters are the minor ($m$) and major ($M$) axis of the ellipse and the azimuthal angle ($\phi$) defined with respect to the $x_1$-axis and $M$. Due to the 2D nature, the azimuthal angle is commonly referred to as the in-plane angle while the out-of-plane angle has been commonly used to refer to $\theta$. Using geometrical principles, the out-of-plane angle is determined by:

$$\theta = \cos^{-1}\left(\frac{m}{M}\right) \tag{6}$$

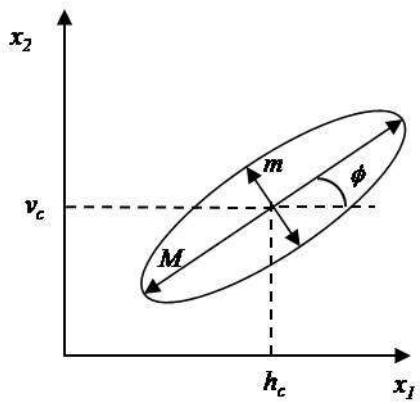


*Figure 2. Definition of five geometrical $v_c$, $h_c$, $m$, $M$, and $\phi$ parameters measured in each ellipses to extract the orientation information.*

## Ambiguity Problem in Short Fiber Orientation

An intrinsic limitation in the method of ellipses is the inability to give complete information about the orientation of the fiber[11]. The problem is that any detected ellipse can represent fibers inclined in two possible directions. Fig. 3 depicts the problem of ambiguity for two fibers with identical ellipses. The perspective views show clearly the differences between these two fibers on a Cartesian coordinate system. However, the geometrical transformation in the method of ellipses requires the use of spherical coordinates which causes the ambiguity. Both fibers have identical out of plane angle, $\theta$; but the in-plane angle is ambiguous because the ellipse cannot distinguish between an in plane angle is $\phi$ or $\phi + \pi$.

The ambiguous angle affects the estimation of some components of the orientation tensor. Consider the analysis for a polished *plane-12* in order to show the effect of ambiguity. After use the Eq. (4), the major components and the $A_{12}$, are completely determined, consequently they are not affected by the ambiguity of $\phi$. However, the sign of the $A_{13}$ and $A_{23}$ orientation components still remain undetermined for every individual fiber.

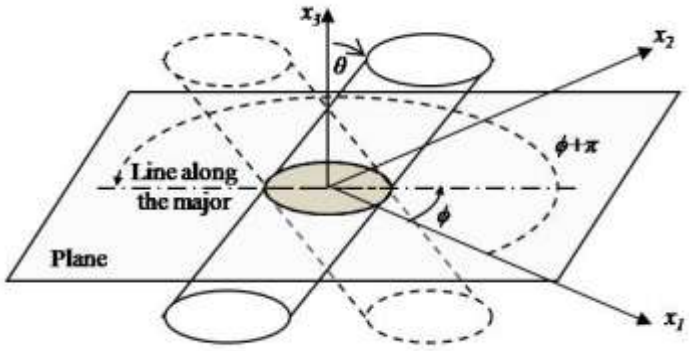


*Figure 3. Ambiguity in fiber orientation. The fiber drawn using continuous line has identical elliptical footprint and out-of-plane angle as the dashed-line fiber, but they differs in out-of-plane angle. $\phi$ and $\phi + \pi$, respectively.*

## Correction of Ambiguity by Using the Methods of Shadows

A controlled plasma etching is used to excavate the polymer matrix surrounding the fibers an exposing their tip. The extreme of the fibers exposed to the air has a dark color that we called shadow and is located at one of the extremes of the major axis of the elliptical footprints. In the proposed method, the presence and location of the shadow is confirmed manually after the step of characterization using the method of ellipses. Fig. 4 can help understand the implementation of the in-plane angle correction based on the location of the shadow. How these shadows are related to a fiber and how the in-plane angle is corrected are shown using a perspective and stop view in Fig 4(a) and (b). As noted in Fig 4(a) when the shadow is located with a shift of $\pi$ ($\phi_s = \phi_m + \pi$ ) with respect to the measured in-plane angle ($\phi_m$), no correction is required ($\phi_{corr} = \phi_m$). However, when in Fig 4(b), the correction of $\phi_{corr} = \phi_m + \pi$ is required because shadow and the measured in-plane angle ($\phi_s = \phi_m$ ). This convention is based on the fact that when a shadow is present, its contour will be located in an underneath or sub-surface plane. No correction in the in-plane angle is introduced when a footprint is absent of shadow or its presence is practically imperceptible.

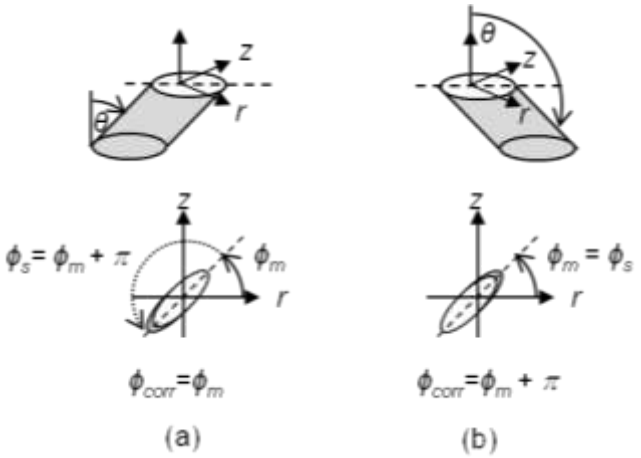


*Figure 4. In-plane angle determination for fiber inclined toward (a) right and (b) left hand side. The in-plane angle for each case is observed on a projection in the rz-plane for each case.*

## Materials and Methods

A 75% short shot center-gated disk of 30wt% short glass fiber PBT with average mass of 18.09 g, average internal diameter ($r_i$) of 2.97 mm, average outer diameter ($R$) of 51.34 mm, and average thickness ($2h$) of 1.39 mm were molded. The filling time of the part was approximately 1 s and the injection pressure was estimated to be 20 MPa. The weighted average length of the fiber was 364$\mu$m.

The disk was cut at several locations, one along a line of constant $\theta$ and three additional cuts tangent to $r$ to obtain specimens containing the initial orientation, 10%, 40% and 90% of ($R$-$r_i$) .The initial orientation of the fibers was experimentally determined at the gate using method of ellipses [4] with a modification to obtain unambiguous orientation. The specimen was metallographically polished in r,z-planes, plasma etched for 40 mins, and gold sputtered. A single-column of images were taken using reflective optical microscopy (20X) with a motorized stage. The images were stitched and the $\phi$ , θ and the relative position of the shadow were obtained using an in-house program written in Matlab. Then, the **A** was computed using Eq (4-5) and the corrections due to the shadow. The orientation was determined in a similar manner along the gapwise direction at 10%, 40% and 90% of ($R$-$r_i$).

## Results and Discussion

### Ambiguity Correction

Correct values of $A_{r\theta}$ are important to completely describe the 3D fiber orientation in the center-gated disk. Values of $A_{\theta z} \approx 0$ were found at all locations in the disk, for this reason is not considered its analysis is not considered in this section. The off-diagonal component $A_{r\theta}$ represents the average tilt of the fibers projected on the $r\theta$- plane, have structural implications. Therefore, three possible conditions can be described by the $A_{r\theta}$ : $A_{r\theta} \approx 0$, $A_{r\theta} > 0$, and $A_{r\theta} < 0$ denoting no tilting, tilting in counter-clockwise direction, and tilting in clockwise direction, respectively. The example illustrated in Fig. 5 can help to understand the structural importance of $A_{r\theta}$. When the ambiguous angle is used the values of are assumed to be positive, which imply that all fibers are tilted in one direction and $A_{r\theta} > 0.30$ as shown in Fig. 5(a). However, when the unambiguous angle is corrected the fibers tend to be tilted in positive and negative directions as shown in Fig. 5(b). Therefore, the distribution of fiber in both direction causes values of $A_{r\theta} \approx 0$.

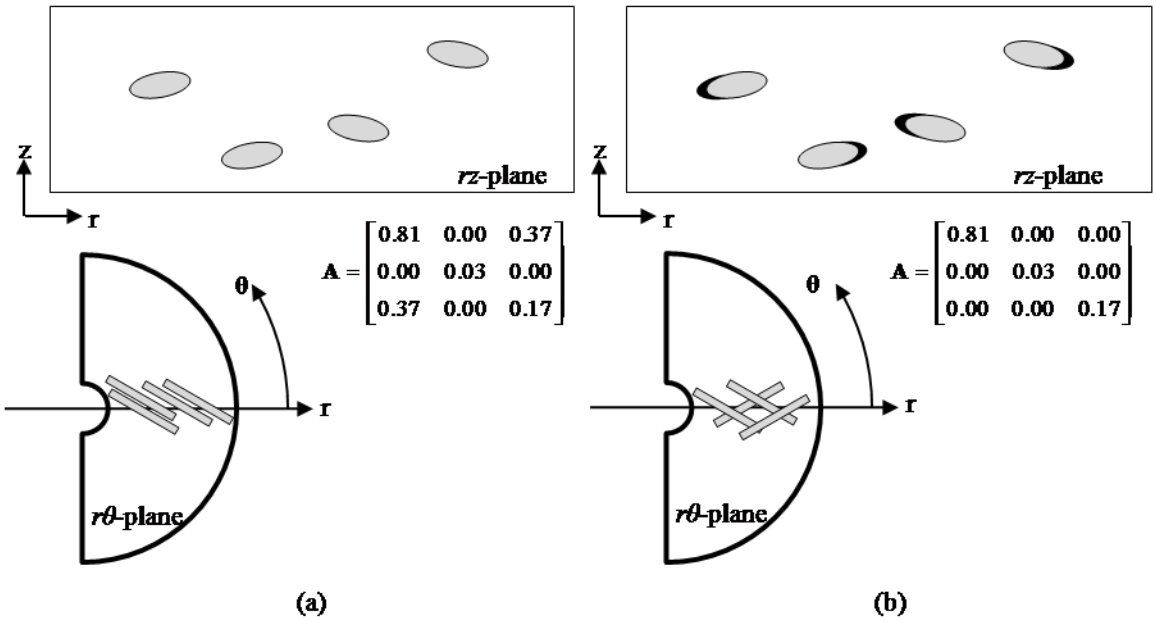


*Figure 5. Structural information related to the $A_{r\theta}$ components based on (a) no correction of the in-plane angle and (b) correction of the in-plane angle using the information of the shadows*

The effect of the ambiguity correction on $A_{r\theta}$ at several radial locations was determined by comparing the orientation obtained using the standard method of ellipses (sMoE) and the proposed method (mMoE). The sMoE approach only takes into account elliptical footprints with ambiguous $\phi$ while mMoE includes all footprints with unambiguous $\phi$. In Fig. 6, a significant difference in $A_{r\theta}$ in the gate region between sMoE and mMoE can be seen at all *z/H* locations. In this figure, the nearly flat orientation profile with approximately constant $A_{r\theta}$ values, i.e. $A_{r\theta} \approx 0.30$ obtained by sMoE contrasts markedly with the asymmetric profile having fluctuations with a mean of $A_{r\theta} \approx 0$ obtained from mMoE. Similar features in $A_{r\theta}$ profiles were found at all radial locations for both sMoE and mMoE approaches.

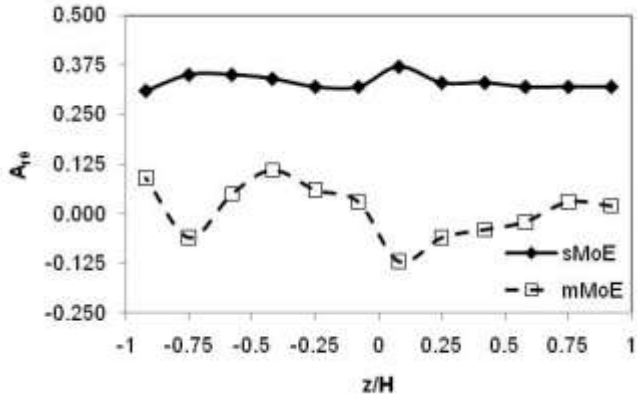


*Figure 6. Effects of ambiguity in $A_{r\theta}$ evaluated by the standard method of ellipses (sMoE) and the proposed (mMoE) approaches at the gate region of a center-gated disk*

## Short Fiber Orientation in a thin center-gated disk

Figure 6 shows the $A_{rr}$ values along the thickness measured at 0%, 10%, 40% and 90% ($R$-$r_i$) for PBT filled with short glass fibers. In this figure, the $A_{rr}$ profile at the gate (0% ($R$-$r_i$)) shows an asymmetric profile that is different than the random orientation profile, typically assumed in numerical simulations of center-gated disc. In addition, several changes in the magnitude and distribution of the $A_{rr}$ compared to the orientation at the gate can be observed as the flow progress. The initial asymmetry fades as a function of the radial location. However, experimental results suggest development of a symmetric orientation or stable structure of orientation for disks at r ≥ 40% ($R$-$r_i$) as postulated by Rao and Altan [8]. Therefore, this observation suggests the formation of a secondary structure of orientation different from the accepted layered structure. This additional structure which evolves from the gate to about 40%R along the flow direction has not been previously reported. The impact of this structure on the mechanical properties can be critical to determine areas of weakness around the gate for large parts, especially when they have multiple gates.

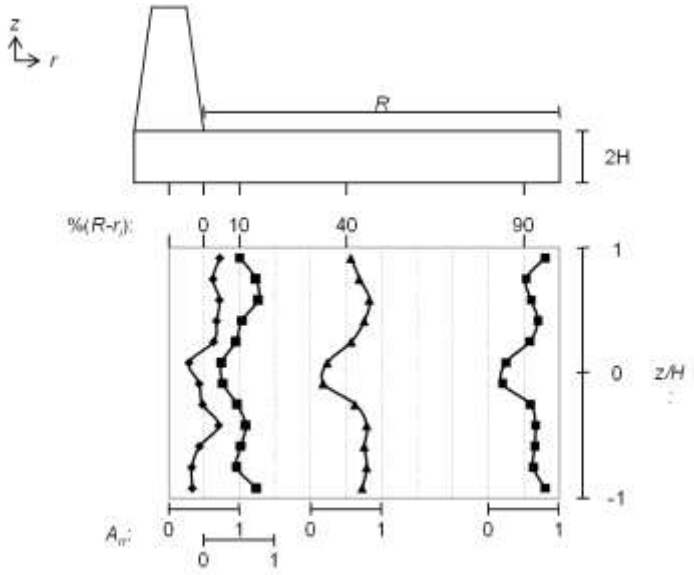


Figure 7. Evolution of orientation in a 75% short shot showing the washout of the asymmetric initial orientation in a center-gated disk.

## Capturing the Flexibility of the Fibers

The assumption of rigidity is not necessarily valid for long fibers. Several theoretical approaches have been developed to model the orientation of long fibers[14,15]. Experimentally, work has been done on the basis of the rigid fiber assumption using the standard method of ellipses, due to simplicity of experiments as well as to utilize the description of the orientation tensor developed short fibers[5,6,16]. Recently, work has been completed utilizing the end-to-end vector to indicate orientation[15]. However, this work presents some limitations in that it assumes a two-dimensional end-to-end vector, whereas this assumption is not necessarily valid in a 3D matrix. Therefore, the three-dimensional orientation as captured by the bead-rod model will be collapsed into an end-to-end vector, so as to maintain the same mathematical description as for short fibers.

The experimental approach is to collect images at multiple planes throughout the depth of the sample. By using the modified method of ellipses for each plane, the 3D projection of the fiber can be established from plane to plane, as shown in Figure 8.

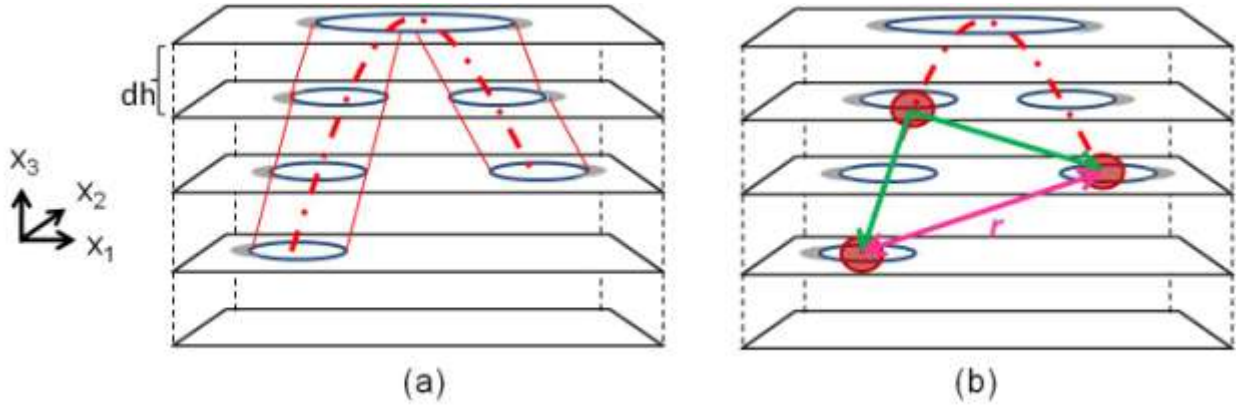


*Figure 8. Representation of a fiber passing through subsequent vertical planes (a), with the red lines serving as visual guides, and (b) the application of the bead-rod and end-to-end vectors for the same fiber*

This experimental approach is currently undergoing testing and evaluation for an end-gated plaque of 1.5 mm thickness. The height of the sample has been differentiated into 15 vertical bins of 100 microns each. The sample will be polished to the center of each bin for image collection, such that the centerline of the sample is located in the middle of the central bin.

Adaptation of the software to combine images from multiple planes is still under development. However, preliminary results show the assumption of rigidity is not valid for long fibers, as shown by the curvature present in Figure 9. A noticeable amount of fiber clustering is also seen. It is unclear at this point if this clustering is resultant of the flow, or as a product of insufficient fiber dispersion prior to injection. The black spaces throughout the image are voids formed within the sample during the molding process.

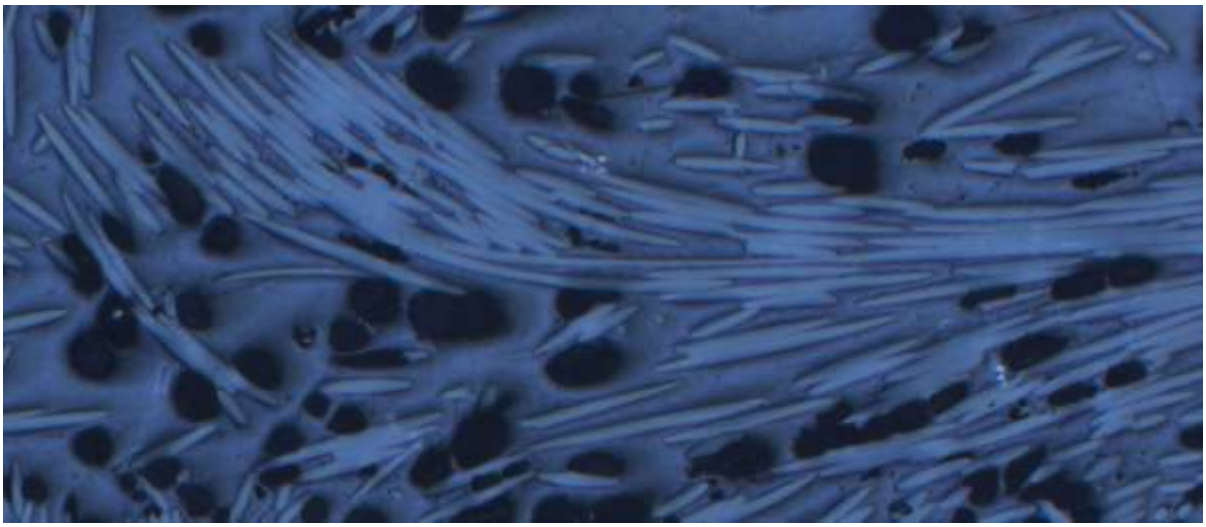

*Figure 9. Image captured of long glass fibers at approximately 90% of the flow direction in a end-gated plaque*

The following image was taken after 60 minutes of plasma etching, which was done to remove a minimal layer of the PP matrix. Figure 10 shows the curvature of several fibers, both in-plane as well as out-of-plane as seen by the elliptical form of the cross-section. The shadows visible at the ends of the ellipses will be used to project the fibers into the subsequent planes below as discussed previously in Figure 8.

*Figure 10. Fiber curvature and shadows at 20X magnification for an end-gated plaque at 90% of the flow-direction*

## Summary

The experimental results indicate that the profile of orientation at the gate was asymmetric and evolved into a steady layered structure of orientation at a radial location larger than 40% of the flow length. This suggests that the typical assumption of initial orientation as a symmetric random profile is not very accurate for a center-gated disk. An asymmetric profile was also found in the $A_{r\theta}$ component at the gate.

A combination of the bead-rod model and end-to-end vector is being evaluated. By imaging a sample at multiple planes throughout the depth, the 3D plane-to-plane projection and orientation of a long fiber can be determined. Imaging software to analyze these multi-plane images concurrently is still under development. However, preliminary results have shown that the rigid rod assumption for long fibers is not valid. The use of the modified method of ellipses via plasma etching and shadow tracking has shown to be possible for analyzing the plane-to-plane images.

## Acknowledgements

The financial support of NSF/DOE: DMI-052918 is gratefully acknowledged. The authors also wish to thank Sabic Americas Inc. for supplying the Valox 420 used in this work. Gregorio M. Vélez-García also acknowledges support from MS&IE-IGERT and University of Puerto Rico-Mayagüez.

## References

1 B Mlekusch, Lehner, EA, Geymayer, W, "Fibre orientation in short-fibre-reinforced thermoplastics - I. Contrast enhancement for image analysis," Compos Sci Technol **59** (4), 543-545 (1999); P.J Hine, Duckett, RA, "Fiber orientation structures and mechanical properties of injection molded short glass fiber reinforced ribbed plates," Polym Composite **25** (3), 237-254 (2004); C.A Silva, Viana, JC, van Hattum, FWJ, Cunha, AM, "Fiber orientation in injection molding with rotating flow," Polym Eng Sci **48** (2), 395-404 (2008).

2 P.F Bright, Crowson, RJ, Folkes, MJ, "A study of the effect of injection speed on fiber orientation in simple mouldings of short glass fibre-filled polypropylene," J Mater Sci **13**, 2497-2506 (1978); M.W Darlington, Smith, GR, "Some features of the injection-molding of short fiber reinforced thermoplastics in center sprue-gated cavities," Polym Composite **8** (1), 16-21 (1987); H. Shen, Nutt, S, Hull, D, "Direct observation and measurement of fiber architecture in short fiber-polymer composite foam through micro-CT imaging," Compos Sci Technol **64** (13-14), 2113-2120 (2004); A. Bernasconi, Cosmi, F, Dreossi, D, "Local anisotropy analysis of injection moulded fibre reinforced polymer composites," Compos Sci Technol **65** (13), 1931-1940 (2008).

3 A.R Clarke, Eberhardt, CN, *Microscopy techniques for materials science.* (CRC, Boca Raton, 2002).

4 R. Blanc, Germain, C, Da Costa, JP, Baylou, P, Cataldi, M, "Fiber orientation measurements in composite materials," Compos Part A-Appl S **37** (2), 197-206 (2006).

5 B.N. Nguyen, Kunc, V,Frame, B, Phelps, JH, Tucker III, CL, Bapanapalli, SK, Holbery, JD, Smith, MT "Fiber length and orientation in long-fiber injection-molded thermoplastics. Part I. Modeling of microstructure and elactic properties," J. Compos. Mater. **42**, 1003–1029 (2009).

6 G.M. Vélez-García, Ortman, KC, Agarwal, N, Wapperom, P, Baird, DG, presented at the SPE Automotive Coposites Conference & Exhibition (ACCE), Troy, MI, 2009 (unpublished).

7 M. Kawamura, Ikeda, S, Morita, S, Sanomura, Y, "Unambiguous determination of 3D fiber orientation distribution in thermoplastic composites using SAM image of elliptical mark and interference fringe.," J Compos Mater **39** (4), 287-299 (2005); G. Zak, Park, CB, Benhabib, B, "Estimation of three-dimensional fibre-orientation distribution in short-fibre composites by a two-section method," J Compos Mater **35** (4), 316-339 (2001).
8 L. Averous, Quantin JC, Lafon D, Crespy A, "Determination of 3D fiber orientations in reinforced thermoplastic using scanning electron microscopy," Acta Stereol **14**, 69-74 (1995).
9 G. Regnier, Dray, D, Jourdain, E, Le Roux, S, Schmidt, FM, "A simplified method to determine the 3D orientation of an injection molded fiber-filled polymer," Polym Eng Sci **48** (11), 2159-2168 (2008).
10 S.G Advani, Tucker, CL "The use of tensors to describe and predict fiber orientation in short fiber composites," J Rheol **31** (8), 751-784 (1987).
11 R.S Bay, Tucker,CL, "Stereological measurement and error estimates for three-dimensional fiber orientation," Polym Eng Sci **32** (4), 240-253 (1992).
12 K.MB Jansen, Van Dijk DJ, Freriksen, MJA, "Shrinkage anisotropy in fiber reinforced injection molded products," Polym Composite **19** (4), 235-334 (1998).
13 N.C Davidson, Clarke, AR, Archenhold, G, presented at the Meeting of Microscopy of Composite Materials III, Oxford, England, 1996 (unpublished); R.S Bay, Tucker,CL, "Fiber orientation in simple injection moldings. 2. Experimental results," Polym Composite **13** (4), 332-341 (1992); B Mlekusch, "Fibre orientation in short-fibre-reinforced thermoplastics - II. Quantitative measurements by image analysis," Compos Sci Technol **59** (4), 547-560 (1999).
14 E. J. Hinch, "The distortion of a flexible inextensible thread in a shearing flow," *J Fluid Mech* **74**, 317-333 (1976); U. Strautins, Latz , A., "Flow-driven orientation dynamics of semi-flexible fiber systems," *Rheol Acta* **46**, 1057-1064 (2007); S. Yamamoto, Matsuoka, T, "A method for dynamic simulation of rigid and flexible fibers in a flow field," J Chem Phys **98**, 644-650 (1993).
15 M. Keshtkar, Heuzey, MC, Carreau, PJ, Rajabian, M, Dubois, C, "Rheological properties and microstructural evolution of semi-flexible fiber suspensions under shear flow," J Rheol **54** (2), 197-222 (2010).
16 P.J. Hine, Davison, N, Duckett, RA, Ward, IM, "Measuring the fibre orientation and modelling the elastic properties of injection-moulded long-glass-fibre-reinforced nylon," Comp Sci Technol **53**, 125-131 (1995).